



**HAL**  
open science

# Electrostatic Energy Harvesting Circuit with DC-DC Converter for Vibration Power Generation System

J Wei, E. Lefeuvre, H. Mathias, François Costa

► **To cite this version:**

J Wei, E. Lefeuvre, H. Mathias, François Costa. Electrostatic Energy Harvesting Circuit with DC-DC Converter for Vibration Power Generation System. *Journal of Physics: Conference Series*, 2016, 773, 10.1088/1742-6596/773/1/012045 . hal-01736133

**HAL Id: hal-01736133**

**<https://hal.science/hal-01736133>**

Submitted on 16 Mar 2018

**HAL** is a multi-disciplinary open access archive for the deposit and dissemination of scientific research documents, whether they are published or not. The documents may come from teaching and research institutions in France or abroad, or from public or private research centers.

L'archive ouverte pluridisciplinaire **HAL**, est destinée au dépôt et à la diffusion de documents scientifiques de niveau recherche, publiés ou non, émanant des établissements d'enseignement et de recherche français ou étrangers, des laboratoires publics ou privés.

PAPER • OPEN ACCESS

# Electrostatic Energy Harvesting Circuit with DC-DC Converter for Vibration Power Generation System

To cite this article: J Wei *et al* 2016 *J. Phys.: Conf. Ser.* **773** 012045

View the [article online](#) for updates and enhancements.

Related content

- [A novel DC-DC converter using LTCC technology for magnetic integration application](#)  
Z Q Xu, Y Shi, H P Guo *et al.*

# Electrostatic Energy Harvesting Circuit with DC-DC Converter for Vibration Power Generation System

J Wei<sup>1a</sup>, E Lefeuvre<sup>a</sup>, H Mathias<sup>a</sup>, F Costa<sup>b</sup>

<sup>a</sup>C2N – CNRS, Univ. Paris Sud/Univ. Paris Saclay, Orsay, France

<sup>b</sup>SATIE – CNRS, Univ. Paris Est Créteil, France

E-mail: jie.wei@u-psud.fr

**Abstract.** This paper presents an interface circuit with power control features for electrostatic vibration energy harvesting. A DC-DC converter is used to control the output voltage of a diode-based charge pump circuit. Therefore, the maximum and minimum voltage across the variable capacitor of the energy harvester may be adjusted to track the maximum power point of the system. The power conversion function of the DC-DC converter depends on the switches configuration. An example of Maximum Power Point Tracking (MPPT) for different conversion function is presented in this paper. Simulation results show that at least 10  $\mu\text{W}$  is generated.

## 1. Introduction

Replacement or recharging of batteries is a major problem for wide development of microscale devices such as wearable electronics, medical implants and wireless sensor networks. Energy harvesting provides a solution. One of the possible power sources in this case is ambient vibration. Electrostatic transduction is a promising way to convert ambient vibrations into electricity. In functional systems, energy harvesting device generally require circuits interface between the harvester and the energy storage element to provide power management function. Since energy harvesting devices produce relatively low output power (often only microwatts), specialized power electronic circuit are necessary.

In this paper, an interface circuit with power control features is presented. It includes a N-cells diode-based interface circuit implementing rectangular charge-voltage cycles [1, 2]. The simplicity and the high efficiency of this interface circuit enabled to implement ultra-low-power electrostatic energy harvesters [3]. However, this diode-based circuit cannot optimize the performance of the system by itself. Due to mechanical damping induced by energy conversion, previous works showed that there exists an optimal operating point at which the output power is maximum [4]. In practice, the operating point can be controlled by adjusting the output voltage value of the N-cells circuit. The association of this circuit with a DC-DC converter enables to achieve this control.

---

<sup>1</sup> To whom any correspondence should be addressed.



**2. Theoretical analysis of the proposed circuit**

The proposed circuit is presented in Figure 1. It consists of an N-cells diode-based interface circuit and a DC-DC converter. The N-cells diode-based interface circuit is used to provide initial charge to the variable capacitor and transfer the generated energy to the storage capacitor (or bulk)  $C_{res}$ . The converter’s input is connected to the  $C_{res}$  and the output is here connected to a rechargeable battery. The start switch is used to provide initial charge to the variable capacitor. The DC-DC converter consists of an inductor and four switches. Its power conversion function depends on the switches configuration and drive.

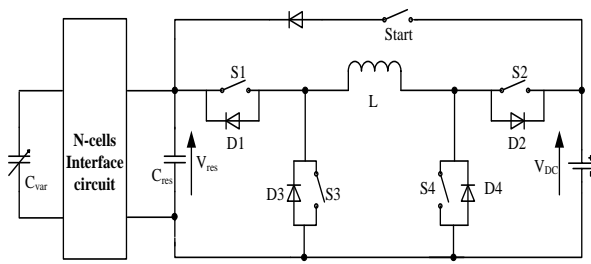


**Figure 1.** Schematic diagram of the proposed circuit

		Controlled switches	State of the rest switches: Open(O) or Closed(C)
Unidirectional	buck	S1	S2(C),S3(O), S4(O)
	boost	S4	S1(C),S2(O), S3(O)
	Buck-boost	S1, S4	S2(O),S3(O)
Reversible	Buck-boost	S1,S2, S3,S4	

**Table 1.** States of switches for different type of converter

Table 1 presents the control of the switches for different possible features. the converter is used to transfer the energy from the storage capacitor to the battery. Hence, the converter function to be used is determined by the optimal voltage range  $[V_{CresL}, V_{CresH}]$  across  $C_{res}$  and the voltage  $V_{DC}$  of the battery. If  $V_{CresL} > V_{DC}$ , a buck converter is required and a boost converter is necessary when  $V_{CresH} < V_{DC}$ . Indeed, they can all be replaced by a buck-boost converter, but with more switches to control, which requires more power to drive the switches. A reversible converter can be also achieved using this generic topology. The use of a reversible converter enables dynamic control of the voltage  $V_{Cres}$  by controlling energy flows between the battery and the capacitor  $C_{res}$  in both directions.

**3. Spice Simulation**

To study the performance of the proposed circuit, an out-of-plan gap-closing MEMS energy harvester [5] was modelled using LTspice software. In the simulations, to get to a high level power range, the gap is modified from 40.5  $\mu\text{m}$  to 81  $\mu\text{m}$  and the mass is changed from 0.066 g to 0.198 g. Figure 2 shows the model schematic of the harvester with a two-cells interface circuit. In this model, the excitation mechanical force is represented as a voltage. The linear mechanical resonator is modeled by a L-C-R circuit, these components representing respectively the inertial mass, the spring compliance and the mechanical damping. The electromechanical coupling is modelled by two behavioral voltage sources. The theoretical expressions of the MEMS capacitance and the electrostatic force as a function of the the displacement  $x$  from the rest position are given respectively by equations (1) and (2).

$$C_{var} = \epsilon * S \left( \frac{1}{d-x} + \frac{1}{d+x} \right) \tag{1}$$

$$F_{elec\_mech} = \frac{1}{2} * V(C_{var})^2 * \left( \frac{1}{(d-x)^2} - \frac{1}{(d+x)^2} \right) \tag{2}$$

In the DC-DC convertor, the ON and OFF states of the electronic switches were modelled by 1  $\Omega$  and 10<sup>10</sup>  $\Omega$  resistors respectively. The switches were operated periodically at 100 kHz with a duty cycle of 50%. The inductor value is 1 mH.

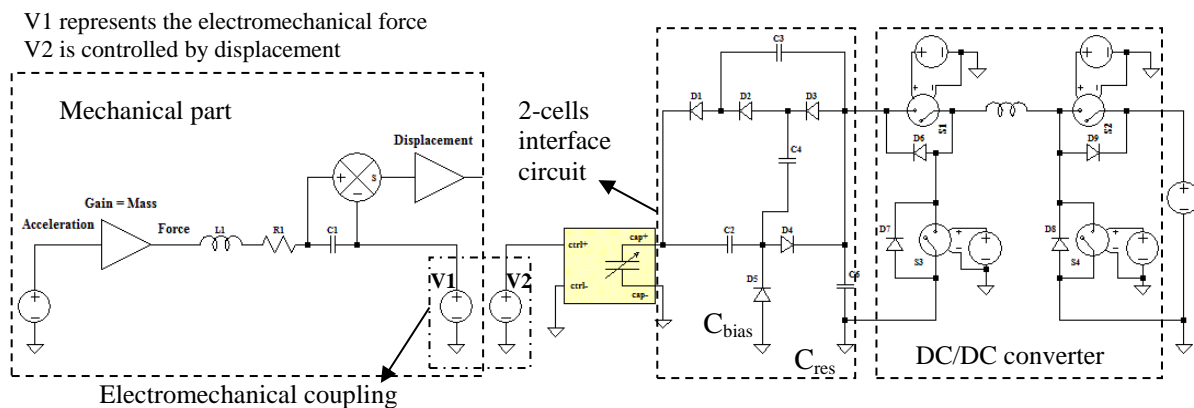


**Figure 2.** LTspice model of the MEMS e-VEH and the proposed circuit

In the simulation, the acceleration was progressively increased at first and then kept constant when it reached  $16 \text{ m/s}^2$ . The waveform of acceleration and the simulation results of power of  $C_{res}$  and  $V_{C_{res}}$ , when all the switches are open, are presented in Figure 3. One can clearly see that there exists an optimal voltage value of  $V_{C_{res}}$  for which the harvested power is maximum. This is due to the electrostatic force, which induces strong damping of the resonator at higher voltages. One can clearly see that the maximum power is  $11 \mu\text{W}$  when  $V_{C_{res}}$  is about  $22\text{V}$ . Choosing a voltage interval of  $V_{C_{res}}$  from  $18\text{V}$  to  $27\text{V}$  enables to get at least 92% of the maximum power.

Simulated waveforms of power of  $C_{res}$  and  $V_{C_{res}}$  with different topologies of converter for MPPT are presented in figure 4. A buck DC-DC converter was connected to a battery of  $10\text{V}$ . Hence, the capacitor  $C_{res}$  was initially charged to  $10\text{V}$ . The converter didn't work with the switches S1, S3, S4 open and S2 closed. After  $45\text{s}$ ,  $V_{C_{res}}$  reached  $27\text{V}$  and the switch S1 was periodically turned on and off with 50% duty cycle at  $100 \text{ kHz}$ . After several cycles,  $V_{C_{res}}$  went down to  $18\text{V}$  and the converter stopped.  $V_{C_{res}}$  came back to  $27\text{V}$  after  $18\text{s}$  and the converter started to work with the switch S1 periodically turned on and off. A boost DC-DC converter was connected to a battery of  $40\text{V}$ . This voltage was too high to start up the system with a weak vibration at the beginning. Hence, at first, to discharge the capacitor  $C_{res}$ , the boost converter worked with S1 closed, S2, S3 open and S4 periodically turned on and off. A reversible converter was also connected to a battery of  $40\text{V}$ . Compared to the boost and buck ones, it had not to use the start switch and the capacitor  $C_{res}$  was able to be charged to any voltage at the beginning. In this simulation,  $V_{C_{res}}$  was initially charged to  $14\text{V}$  with the switches S2, S3 open and the switches S1, S4 periodically turned on and off with 50% duty cycle at  $100\text{kHz}$ . After  $45\text{s}$ ,  $V_{C_{res}}$  was discharged when the switches S1, S4 open and the switches S2, S3 periodically turned on and off. For the 3 different topologies of converter, one can clearly see that at least  $10 \mu\text{W}$  is generated.

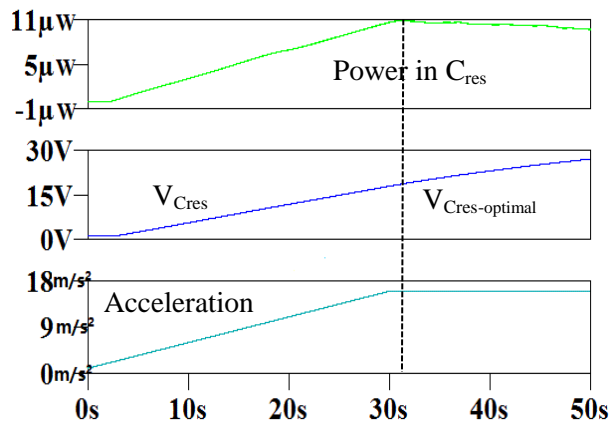


**Figure 3. Simulated power in  $C_{res}$ ,  $V_{Cbias}$ , and  $V_{Cres}$  vs time**

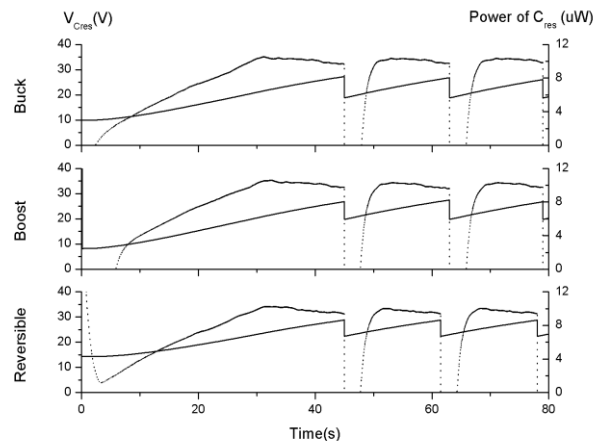


**Figure 4. Simulated waveforms of power in  $C_{res}$  (dotted lines) and  $V_{Cres}$  (solid lines) with different topologies of converter for MPPT**

#### 4. Conclusion

This interface circuit for electrostatic energy harvesters enables to adjust the voltage across the variable capacitor to optimize the performance of the system. Simulation results show that Tracking of maximum power point is achievable for different functions of DC-DC converter. Our future work will focus on the strategy of switch control and on the design of the integrated control circuit.

#### 5. Reference

- [1] De Queiroz A C M, Domingues M 2011 the doubler of electricity used as battery charger IEEE Trans. Circ. Syst. II: Express Briefs 58(12) pp 797-801
- [2] Lefeuvre E, Risquez S, Wei J, Woytasik M, Parrain F 2014 Self-Biased Inductor-less Interface Circuit for Electret-Free Electrostatic Energy Harvesters J. Phys.: Conf. Series 557 012052.
- [3] Wei J, Risquez S, Mathias H, Lefeuvre E, Costa F 2015 Simple and Efficient Interface Circuit for Vibration Electrostatic Energy Harvesters Proc. IEEE Sensors Conf. 2015
- [4] Dorzhiev V, Karami A, Basset P et al. MEMS electrostatic vibration energy harvester without switches and inductive elements. Journal of Physics: Conference Series 557 (2014) 012126.
- [5] Basset P, Galayko D, Cottone F, Marty F, Dudka A, Bourouina T 2014 Electrostatic vibration energy harvester with combined effect of electrical nonlinearities and mechanical impact J. Micromech. Microeng. 24 035001

#### Acknowledgments

This work is supported by the “IDI 2014” project funded by the IDEX Paris-Saclay, ANR-11-IDEX-0003-02